Chloroperoxidase Compound I: Electron Paramagnetic Resonance and Mössbauer Studies†

Rick Rutter,‡ Lowell P. Hager,* Howard Dhonau, Michael Hendrich, Mark Valentine,§ and Peter Debrunner

ABSTRACT: The green primary compound of chloroperoxidase was prepared by freeze-quenching the enzyme after rapid mixing with a 5-fold excess of peracetic acid. The electron paramagnetic resonance (EPR) spectra of these preparations consisted of at least three distinct signals that could be assigned to native enzyme, a free radical, and the green compound I as reported earlier. The absorption spectrum of compound I was obtained through subtraction of EPR signals measured under passage conditions. The signal is well approximated by an effective spin $S^{eff} = {}^1/_2$ model with $\mathbf{g} = 1.64, 1.73, 2.00$ and a highly anisotropic line width. Mössbauer difference spectra of compound I samples minus native enzyme showed well-resolved magnetic splitting at 4.2 K, an isomer shift $\delta_{Fe} = 0.15$ mm/s, and quadrupole splitting $\Delta E_Q = 1.02$ mm/s. All data are consistent with the model of an exchange-coupled spin $S = 1$ ferryl iron and a spin $S' = {}^1/_2$ porphyrin radical. As a result of the large zero field splitting, D, of the ferryl iron and of intermediate antiferromagnetic exchange, $\vec{S}\cdot\mathbf{J}\cdot\vec{S}'J \sim 1.02$ D, the system consists of three Kramers doublets that are widely separated in energy. The model relates the EPR and Mössbauer spectra of the ground doublet to the intrinsic parameters of the ferryl iron, $D/k = 52$ K, $E/D \simeq 0.035$, and $A_\perp/(g_n\beta_n) = 20$ T, and the porphyrin radical. The magnitude of D was deduced from the temperature-dependent half-saturation power of the EPR signal, which showed that an Orbach transition to the second Kramers doublet dominates the longitudinal spin relaxation rate for $T > 5$ K. The spin-coupling model is shown to account for all green primary compounds studied so far.

The peroxidase family of enzymes is dominated by heme proteins that catalyze the following generalized reaction sequence:

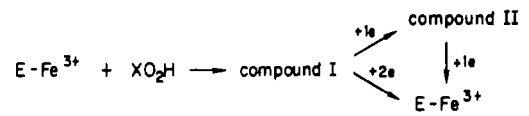

In this sequence, E–Fe^{3+} represents the native, ferric enzyme; XO_2H is the peroxide substrate, where X can be a proton, methyl, ethyl, aceto, or other organic group; compounds II and I represent forms of the enzyme that are more oxidized than the resting enzyme by one (II) and two (I) electrons, respectively. Oxidized peroxidases can return to their resting state by reacting sequentially with one-electron donors. Horseradish peroxidase compound I, for example, usually uses two one-electron donors to return to the native state. On the other hand, compound I can react with a two-electron donor and return directly to the resting state. This reaction is exemplified by chloroperoxidase, which utilizes a halide ion as a two-electron donor to form an oxidized halide–enzyme intermediate. This halide–enzyme intermediate (Shaw & Hager, 1961; Libby et al., 1982) then halogenates an organic nucleophile, and the enzyme returns to its native resting state.

The chemical nature of the higher oxidation states of the peroxidase intermediates has been the center of recent interest. Model compound studies (Dolphin et al., 1971) and the combined results of optical (Palcic et al., 1980; DiNello & Dolphin, 1981), Mössbauer (Lang et al., 1976; Schulz et al., 1979a), NMR (LaMar & de Ropp, 1980), EPR (Schulz et al., 1979b), and ENDOR spectroscopy (Roberts et al., 1981a, Hoffman et al., 1979) on primary and secondary peroxidase compounds have led to basic insights into the electronic structure of these intermediates.

All recent studies on peroxidase compounds I and II indicate that the iron atom of the heme prosthetic group exists in an oxyferryl state, OFe^{IV}, in both of these intermediates. The strongest evidence for a $(3d)^4$ Fe(IV) configuration in these compounds comes from the isomer shifts observed in Mössbauer spectra, $0.03 \text{ mm/s} \leq \delta \leq 0.15$ mm/s (Lang et al., 1976; Schulz et al., 1979a,b, 1984). The ferryl assignment accounts for the 1 oxidizing equiv associated with compound II; however, since the primary compounds contain 2 oxidizing equiv, an additional oxidized species must exist either on the porphyrin or on an amino acid residue in the protein. The primary compounds have an odd number of electrons and are, therefore, Kramers systems that can be expected to be EPR active. An organic radical-type EPR signal has long been known to be associated with the red compound ES of cytochrome *c* peroxidase (Yonetani et al., 1966). However, it has only recently been possible to detect and quantitate the EPR signal associated with the green compound I intermediate, which is the more common two-electron-oxidized species found in the peroxidase family. The compounds I of horseradish and chloroperoxidase give very broad EPR spectra that quantitate to approximately one unpaired electron per heme group (Schulz et al., 1979b; Rutter & Hager, 1982). It is now evident that the green color of the primary compounds is characteristic of porphyrin π cation radicals in which one of the porphyrin π electrons has been removed to leave an unpaired spin of $S' = {}^1/_2$. In contrast, the red compound ES of cytochrome *c* peroxidase is created by the removal of an electron from an amino acid residue at some distance from the ferryl prophyrin.

The broad EPR signal associated with the green compound I intermediates results from the exchange interaction

$$\hat{\mathcal{H}}_{ex} = \hat{S}\cdot\mathbf{J}\cdot\hat{S}' \quad (1)$$

between the ferryl iron of spin $S = 1$ and the porphyrin radical

† From the Departments of Biochemistry and Physics, University of Illinois, Urbana, Illinois 61801. *Received May 31, 1984.* Supported in part by USPHS Grants GM 16406 and GM 07768 and NSF Grant PCM-8209325.

‡ Present address: Monsanto Co., St. Louis, MO 63167.

§ Present address: Gray Freshwater Biological Institute, Navarre, MN 55392.

0006-2960/84/0423-6809$01.50/0

of spin $S' = {}^1/_2$. This exchange interaction was proposed by Schulz et al. (1979b) to explain the EPR signal centered at $g = 2$ for horseradish peroxidase compound I. Subsequent ENDOR experiments confirmed that the broad EPR signal is associated with the porphyrin radical (Roberts et al., 1981a). Furthermore, these studies showed that an oxygen atom from $H_2{}^{17}O_2$ remains bound to the iron atom of horseradish peroxidase compound I (Roberts et al., 1981b).

Chloroperoxidase differs in many respects from horseradish and cytochrome *c* peroxidase. In addition to its specific chlorination reaction, it possesses classical peroxidase and high catalase activities. Chloroperoxidase also shares many spectral features with the P-450 cytochromes in several of its stable states (Champion et al., 1973, 1975), presumably as a result of a sulfur axially coordinated to the heme iron (Cramer et al., 1978). The existence of a compound I type intermediate has also been postulated in the reaction cycle of cytochrome P-450 (Dolphin, 1981; Wagner & Gunsalus, 1981). Thus, a detailed study of chloroperoxidase compound I is desirable from both the peroxidase and cytochrome P-450 points of view. In contrast to the primary compounds of horseradish and cytochrome *c* peroxidase, chloroperoxidase compound I is quite unstable, and no compound II state has been isolated so far.

The optical spectrum of chloroperoxidase compound I resembles that of catalase compound I (Palcic et al., 1980) and is quite different from that of horseradish peroxidase compound I. A broad EPR signal with g values $g_\parallel \sim 1.99$ and $g_\perp \sim 1.73$ has been recorded for chloroperoxidase compound I (Rutter & Hager, 1982). In this paper we present rapid passage and power saturation EPR studies on freeze-quenched samples of chloroperoxidase compound I together with Mössbauer spectra of ^{57}Fe-enriched chloroperoxidase compound I. We extend the spin-coupling model proposed for horseradish peroxidase compound I by Schulz et al. (1979b) and show that it accounts quantitatively for the chloroperoxidase compound I data. The effective magnetic moments of the green primary compounds differ considerably from system to system depending on the sign of $\hat{\mathcal{H}}_{ex}$, eq 1, and its magnitude relative to the zero field splitting $\hat{\mathcal{H}}_0$

$$\hat{\mathcal{H}}_0 = D(\hat{S}_z{}^2 - 2/3) + E(\hat{S}_x{}^2 - \hat{S}_y{}^2) \qquad (2)$$

While horseradish compound I illustrates the case of weak coupling, $|J|/D \leq 0.1$, and a recent model compound the case of strong, ferromagnetic coupling, $-J/D \gg 1$ (Boso et al., 1983), chloroperoxidase compound I is a case of intermediate, antiferromagnetic coupling, $J/D \sim 1$. Of all the ferryl states studied thus far, chloroperoxidase compound I has the largest zero field splitting, $D/k \sim 52$ K, the largest isomer shift, $\delta_{Fe} = 0.15$ mm/s, and the smallest quadrupole splitting, $\Delta E_Q = 1.02$ mm/s.

Materials and Methods

Chloroperoxidase was purified from culture filtrates of *Caldariomyces fumago* that had been grown in the presence of fructose as the sole carbon source (Pichard, 1981). Purification was carried out according to the procedure developed by Morris & Hager (1966) with the slight modifications described previously (Palcic et al., 1980). The purity of chloroperoxidase samples was routinely determined by measuring the R_z value (absorbance at 399 nm/absorbance at 280 nm). Enzyme concentrations were determined with an extinction coefficient of 8.5×10^4 M^{-1} cm^{-1} at 399 nm. Visible absorption spectra were recorded on a Cary 219 spectrophotometer.

Stock solutions of peroxide were assayed by measuring the formation of triiodide ion, I_3^-, from potassium iodide in the presence of horseradish peroxidase as the catalyst (Cotton et al., 1973). Peracetic acid was obtained as a 40% solution from FMC Corp.

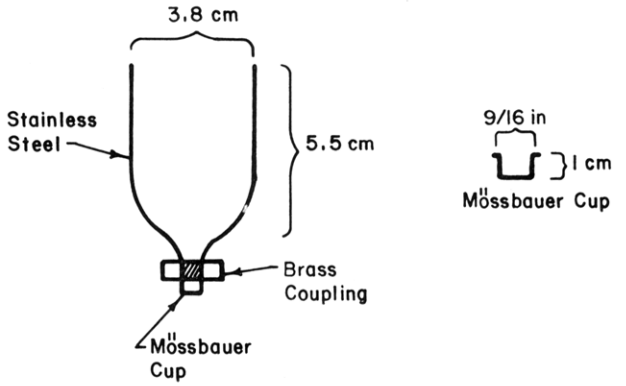

FIGURE 1: Collection cup and Mössbauer cell used in the preparation of samples by freeze-quenching.

EPR measurements were performed on a Bruker ER 200D X-band spectrometer equipped with an Oxford ESR 10 helium-flow cryostat and DTC-2 temperature controller. The temperature uniformity along the EPR sample tube was greatly improved by the addition of a metal-extension dewar. Tests with three carbon resistors placed in an EPR tube showed that the temperature gradient was less than 0.2 K/cm under the experimental conditions, which was adequate for the measurements of the half-saturation power. The spectrometer was interfaced with an LSI 11/23 computer for data storage and manipulation.

The Mössbauer spectrometer was of the constant-acceleration type. The Doppler shift was calibrated periodically with an iron foil that also served to establish the reference point for the isomer shift δ_{Fe}. The Mössbauer samples were maintained at constant temperature in a Janis helium-flow cryostat.

EPR freeze-quench samples were prepared by the method of Ballou & Palmer (1974) with a Precision Ram Instrument from Update Instruments Co. Mössbauer freeze-quench samples were prepared in a stainless steel collection cup 3.8 cm in diameter and 5.5 cm high to which a 0.5- or ${}^9/_{16}$-in. diameter Mössbauer cup was attached by means of a threaded brass seat (Figure 1). The lip on the Mössbauer cup shown in Figure 1 fits into the brass coupling so that it is seated firmly against the collection cup. The freeze-quench assembly was placed in a dewar flask containing isopentane at a temperature of −140 °C. The quenched reactants were packed into the Mössbauer cup with a 0.5-in. diameter nylon rod. The Mössbauer cup was then removed from the cold isopentane bath and stored in liquid N_2. EPR and Mössbauer freeze-quench samples were routinely prepared from enzyme concentrations between 0.75 and 3.6 mM. The molar ratio of peracetic acid to enzyme was generally 5 to 1.

EPR saturation data were collected by measuring the EPR absorption derivative signal intensity as a function of microwave power at different temperatures. The saturation data were fitted to the expression

$$S/P^{1/2} \propto 1/(1 + P/P_{1/2})^{1/2} \qquad (3)$$

where S is the derivative signal intensity, P is the microwave power, and $P_{1/2}$ is the half-saturation power. A nonlinear least-squares fit to eq 3 yielded a $P_{1/2}$ value for each particular temperature.

Results

EPR Studies on Chloroperoxidase Compound I. We studied freeze-quenched samples of chloroperoxidase com-

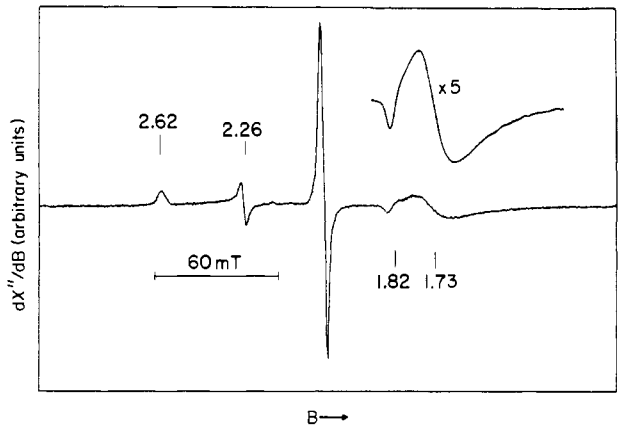

FIGURE 2: EPR spectrum of chloroperoxidase compound I at 3.5 K. The freeze-quenched sample of 2.5 mM protein in 50 mM phosphate/citrate buffer, pH 3.4, contained 45% native enzyme, $g = 1.82$, 2.26, 2.62, and 55% compound I, $g_\perp \sim 1.73$ and $g_\parallel = 2$. The absorption derivative shown was recorded at 9.5 GHz with a power of 20 μW, 100-kHz modulation of 2-mT amplitude, and a sweep rate of 2 mT/s.

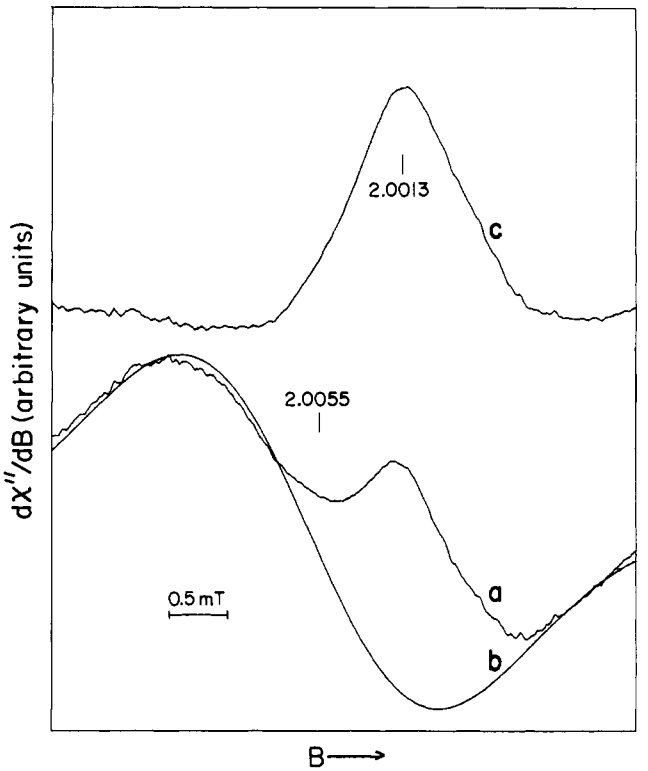

FIGURE 3: EPR spectrum of the $g = 2$ feature of compound I at 3.5 K. Trace a was obtained with the same sample and the same conditions as in Figure 2 except for the smaller modulation amplitude of 0.2 mT and sweep rate of 50 μT/s. Trace b is a Gaussian simulation of the radical impurity at $g = 2.0055$ with a peak-to-peak line width of 2.2 mT. Trace c is the difference between (a) and (b); it represents the low-field edge at $g = 2.0$ of the compound I signal.

pound I by EPR under various experimental conditions. In addition to the novel chloroperoxidase compound I signal with $g_\parallel \sim 1.99$ and, $G_\perp \approx 1.73$, we observed variable admixtures of the low-spin ferric signal with $\mathbf{g} = 2.62$, 2.26, 1.82 arising from resting enzyme, a $g = 4.22$ signal, and a free radical species of $g \approx 2$. In order to construct the true compound I spectrum, we subtracted the low-spin ferric signal arising from native enzyme, which partially overlaps with the compound I spectrum. The radical with $g \simeq 2$ is independent of the broad chloroperoxidase compound I EPR signal. This conclusion follows from the fact that the $g \simeq 2$ signal saturates

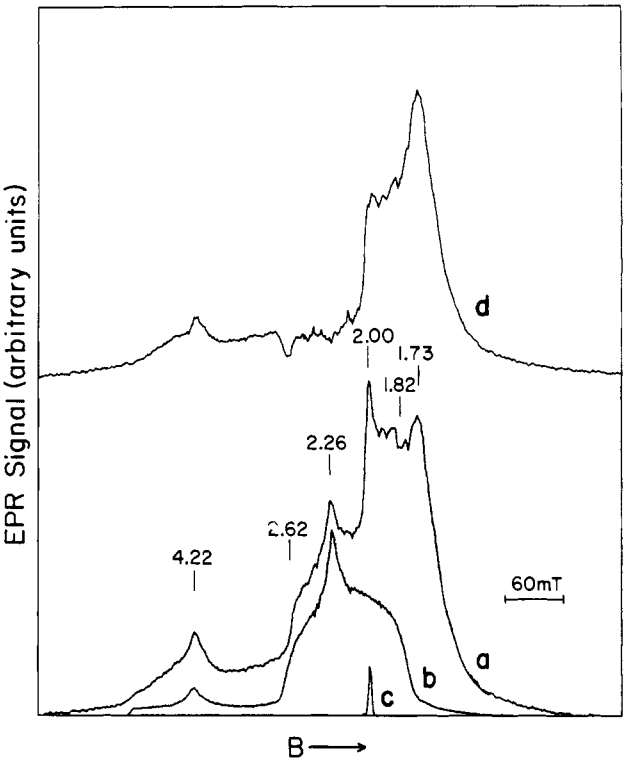

FIGURE 4: EPR absorption spectrum of compound I at 3 K. Trace a is an absorption-type spectrum of the sample in Figure 2 obtained in the dispersion mode under rapid passage conditions with 2-mW microwave power at 9.5 GHz, 100-kHz modulation of 0.16-mT amplitude, and a sweep rate of 3.5 mT/s. Trace b is the properly scaled spectrum of a native chloroperoxidase sample recorded under the same conditions as in (a). Trace c was obtained with the sample of Figure 2 under similar conditions as in (a) except that the temperature was raised to 73 K, where the heme signals are negligible and only the radical signal is seen. Spectrum d is the difference (a) − (b) − (c) and represents the absorption-type signal of compound I. The impurity spectra b and c were scaled to yield the most plausible difference spectrum d.

at lower power levels and is observable at much higher temperatures than the $g_\parallel \simeq 2$ and $g_\perp \approx 1.73$ signal. Figure 2 shows an unsaturated derivative spectrum obtained from a compound I sample that contained 45% of contaminating native enzyme. The chloroperoxidase compound I signal extends from ~0.33 to 0.45 T; its low-filed edge gives rise to a positive derivative peak near $g = 1.99$, which is partially hidden by the positive and negative spikes due to the radical signal. A spectrum of the $g = 2$ region was recorded with higher resolution in Figure 3, which allowed separation of the two components. The low-field g value of compound I is found to be $g = 2.0013$ whereas the radical has $g = 2.0055$ and a peak-to-peak width of 2.2 mT. Under the conditions of the experiment the satellites of the radical reported by Rutter & Hager (1982) are not resolved.

It is possible to observe an absorption-type spectrum, as shown in Figure 4a, by using nonadiabatic rapid passage conditions in the dispersion mode.[1] In Figure 4d, the EPR

[1] Weger (1960) has classified passage conditions on the basis of the quantities dB_0/dt, B_1, B_m, and ω_m, which are experimentally adjustable, of the relaxation times T_1 and T_2, which decrease with temperature, and of the (inhomogeneous) line width ΔH, which is ~60 mT for chloroperoxidase compound I. The experimental conditions as specified in the caption of Figure 4 correspond to Weger's case 10 if we assume that T_1 and T_2, which have not been measured for chloroperoxidase compound I, are comparable to those of horseradish peroxidase compound I, T_1(3 K) ~ 52 ms ~ $3 \times 10^3 T_2$ (Colvin et al., 1983). The spin fluctuation model of the Mössbauer line shape (footnote 7) leads to an estimate of T_1(3 K) > 50 ms.

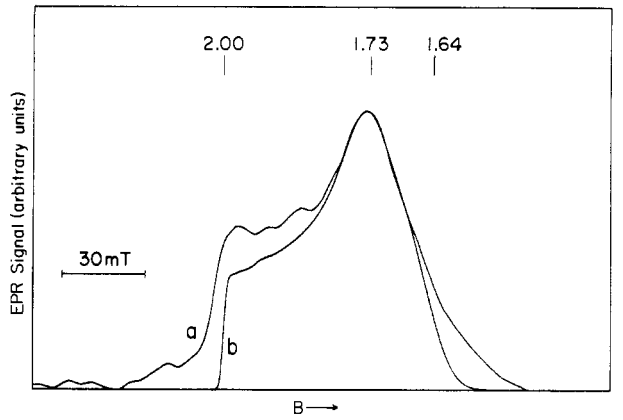

FIGURE 5: EPR absorption spectrum of compound I after correction. Trace a is the relevant part of the corrected spectrum Figure 4d after expansion and smoothing. Trace b is a simulation based on the spin-coupling model, eq 7, with D/k = 52 K, E/D = 0.035, J/k = (52, 52, 54)K, and $\mathbf{g}$ = 2.265, 2.295, 1.96, g' = 2.08. The line width is modeled by allowing $\mathbf{J}$ to have a Gaussian distribution about the specified principal axes values with a standard deviation $\sigma(J)/k$ = 1.14 K and assuming a minimum width of 1 mT. An almost indistinguishable simulation is obtained with an effective spin $S^{eff} = {}^1/_2$ model, an effective g tensor $\mathbf{g}^{eff}$ = 1.62, 1.73, 2.0, and a line-width tensor w = (17.5, 17.5, 5) mT.

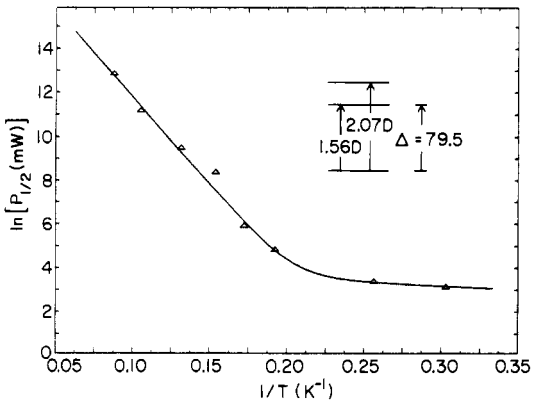

FIGURE 6: Half-saturation power $P_{1/2}$ as a function to temperature. The $P_{1/2}$ values were obtained from least-squares fits to eq 1 of the signal S as a function of microwave power P at each temperature. The signal S was the peak to peak absorption derivative measured at g = 1.73. The solid line is a fit of the logarithm of $P_{1/2}$ according to eq 2; it indicates that for $T > 5$ K the spin–lattice relaxation is dominated by Orbach transitions to an excited Kramers doublet at Δ = 79.5 K. The insert shows the three Kramers doublets of the spin-coupled ferryl porphyrin radical complex.

signals from native chloroperoxidase, Figure 4b, and from the radical, Figure 4c, have been removed by subtraction. The difference spectrum, Figure 4d, still contains impurities, mainly because the sample of native chloroperoxidase, which yielded Figure 4b, contained less of the g = 4.22 signal than the compound I sample. Sample Figure 4a was recorded under strongly saturating conditions, the radical signal, Figure 4c, is small; the amount subtracted was adjusted to give a difference spectrum compatible with the absorption derivative in Figure 3c. The main features of the compound I signal are brought out more clearly in Figure 5a, which was obtained from Figure 4d by truncation and smoothing. Figure 5b is a computer simulation based on the spin-coupling model to be discussed later.

We also studied the saturation behavior of the compound I signal in order to determine the temperature dependence of its spin–lattice relaxation time T_1. According to our model, the spin of the porphyrin radical couples with the ferryl spin triplet, which has a large, positive zero field splitting parameter D. The resulting system consists of three Kramers doublets, the lowest one of which is EPR active. The higher doublets largely determine the spin relaxation rate $1/T_1$ of the ground doublet because they allow two-phonon Orbach processes, $1/T_1 \propto 1/(\exp[E/(kT)] - 1)$, which dominate over the one-phonon direct process, $1/T_1 \propto T$, at all but the lowest temperatures. The observation of an Orbach process not only confirms our model, but it also allows the determination of the energies E_1 and E_2 of the higher doublets. In Figure 6 we plot the logarithm of the half-saturation power $P_{1/2}$, which is defined in eq 3, against $1/T$. The data are well fitted by the function (Yim et al., 1982)

$$P_{1/2} = AT + B/[\exp(\Delta/T) - 1] \qquad (4)$$

with A = 7.15 μW/K, B = 380 W, and Δ = 79.5 K. Orbach transitions to the highest Kramers doublet are much less efficient than the transition to the intermediate doublet in relaxing the ground doublet; thus, $k\Delta$ must be close to the energy E_1 of the latter.[2]

Mössbauer Studies on Chloroperoxidase Compound I. We recorded Mössbauer spectra of several freeze-quenched samples of ^{57}Fe-enriched chloroperoxidase compound I. Native chloroperoxidase, which was found to be a significant contaminant in all preparations, was studied separately under identical experimental conditions. The spectra of the native enzyme were essentially the same as reported earlier[3] (Champion et al., 1973) and were not noticeably affected by the freeze-quench procedure. Figure 7 shows the spectra of chloroperoxidase compound I at 4.2 K after subtraction of an appropriate amount (~30% of original area) of the native enzyme component. Since the latter extends from −6 to 5 mm/s, i.e., far beyond the range of ±3 mm/s covered by chloroperoxidase compound I, the fraction to be subtracted is readily determined by the condition that the corrected spectrum reaches background level for Doppler shifts $|v| > 3$ mm/s. Apart from the small isomer shift, δ_{Fe} = 0.15 mm/s, which is characteristic of the ferryl heme state, the most striking features of the spectra in Figure 7a,b are the well-resolved magnetic hyperfine splittings and the fact that the direction of the 34-mT applied field strongly affects the line intensities. This last point indicates that the iron is associated with the EPR signal. Under the same experimental conditions, horseradish peroxidase compound I shows much weaker magnetic interaction giving rise to some broadening of the quadrupole-split pair of lines. No further changes in the chloroperoxidase compound I spectra are observed when the temperature is lowered, but when the temperature is raised above 15 K, a quadrupole doublet emerges with a splitting ΔE_Q = 1.02 mm/s.

Since the iron is associated with the EPR signal, we may use an effective spin $S^{eff} = {}^1/_2$ Hamiltonian to simulate the Mössbauer spectra

[2] Since the lattice vibrations couple strongly to the spin S = 1 of the iron but not to the porphyrin radical, $S' = {}^1/_2$, the latter relaxes only via the exchange coupling to the iron. As a result, transitions to the highest Kramers doublet do not contribute significantly to the relaxation of the ground doublet. If one uses a spin fluctuation model of the Mössbauer line shape (Schulz & Debrunner, 1984) and the fact that the magnetic hyperfine splitting collapses between 15 and 30 K, the spin fluctuation rate parameter is estimated to be $W_0 = 7.3 \times 10^3$ rads^{-1} K^{-3}, which leads to $T_1 \sim 42$ ms at 4.2 K.

[3] In contrast to the new preparations, the older ones contained a Mn impurity, which gave rise to an EPR signal near g = 2 and could, in principle, interact with the heme iron. We conclude that any such interaction must have been negligible, since the Mössbauer spectra taken in an applied field of 130 mT are indistinguishable in the old and the new samples.

$$\hat{\mathcal{H}}^{\text{eff}} = \beta \hat{S}^{\text{eff}} \cdot \mathbf{g}^{\text{eff}} \cdot \hat{B} + \hat{S}^{\text{eff}} \cdot \mathbf{A}^{\text{eff}} \cdot \hat{I} + \hat{\mathcal{H}}_Q \quad (5)$$

where $\mathbf{g}^{\text{eff}}$ is the effective $\mathbf{g}$ tensor determined by EPR, $\mathbf{A}^{\text{eff}}$ is an effective magnetic hyperfine tensor

$$\hat{\mathcal{H}}_Q = (eQV_{zz}/12)[3\hat{I}_z^2 - 15/4 + \eta(\hat{I}_x^2 - \hat{I}_y^2)] \quad (6)$$

the quadrupole interaction of the $I = {}^3/_2$ nuclear excited state, and $\eta = (V_{xx} - V_{yy})/V_{zz}$ is the asymmetry parameter. From spectra taken at $T \geq 30$ K, we know the quadrupole splitting $\Delta E_Q = (eQV_{zz}/2)(1 + \eta 2/3)^{1/2} = 1.02$ mm/s. The solid lines in Figure 7a,b are obtained with axially symmetric tensors $\mathbf{g}^{\text{eff}}$, $\mathbf{A}^{\text{eff}}$, V_{ii}, and $\eta = 0$, $A_\perp/(g_n\beta_n) = -30$ T, and $A_\parallel/(g_n\beta_n) = -6$ T, taking $A_\parallel$ and V_{zz} parallel to $g_\parallel$. The Mössbauer data do not rule out moderate deviations from axial symmetry. We note that the simulation predicts less absorption near $v = -1$, 0.3, and 1.2 mm/s than is shown by the data; the difference spectrum c = b − a, however, is matched quite well. We conclude that the Mössbauer sample contains at least one, and most likely two, further admixtures that is(are) not affected by the direction of the 34-mT applied field. The chemical nature of the admixtures has not been determined.[4]

Discussion

The following common features of the heme electronic structure emerge from the optical, magnetic, and Mössbauer studies of the green primary compounds of horseradish and chloroperoxidase: (i) The heme iron is in $(3d)^4$, $S = 1$ configuration with a tightly bound oxygen atom (Hager et al., 1972; Roberts et al., 1981b). This oxoferryl state is also found in horseradish peroxidase compound II and compound ES of cytochrome *c* peroxidase; it is characterized by a large axial zero field splitting, eq 2, $D/k \geq 30$ K, and by a specific range of isomer shifts, axial quadrupole, and magnetic hyperfine interactions (Schulz et al., 1984). The ferryl state can be described by a crystal field model (Oosterhuis & Lang, 1973) or, to a good approximation, by the simpler spin Hamiltonian formalism. (ii) An electron is missing from the highest occupied porphyrin orbital of the heme prosthetic group in the enzyme. Thus, the prophyrin is oxidized to a pi cation radical that has an optical absorption markedly different from that of the normal heme group (Dolphin et al., 1971). The heme complex has an odd number of electrons and therefore should give an EPR signal. (iii) The spins $S = 1$ of the ferryl iron and $S' = {}^1/_2$ of the porphyrin radical are coupled to give three kramers doublets. The lowest one of these doublets can be probed by EPR and Mössbauer measurements at low temperature; the higher ones can be inferred from Orbach spin relaxation processes. The properties of the lowest doublet depend on the spin–spin interactions as well as on the intrinsic properties of the ferryl iron and porphyrin. We will show that the striking differences between chloroperoxidase compound I and horseradish peroxidase compound I in their EPR and Mössbauer spectra are mainly due to the stronger exchange interactions in chloroperoxidase compound I.

Following Schulz et al. (1979), we model the coupling between the ferryl spin $S = 1$ and the spin $S' = {}^1/_2$ of the porphyrin radical by the phenomenological exchange interaction $\hat{\mathcal{H}}_{ex} = \hat{S} \cdot \mathbf{J} \cdot \hat{S}'$, eq 1, where the 3×3 components of the tensor $\mathbf{J}$ are adjustable parameters. Often it will be sufficient to consider the simpler case of isotropic exchange $\hat{\mathcal{H}}_{ex} = J\hat{S} \cdot \hat{S}'$ where J is a scalar.[5] We assume that the electronic state of the complex can be described by the Hamiltonian

$$\hat{\mathcal{H}} = \hat{\mathcal{H}}_0 + \hat{\mathcal{H}}_{ex} + \hat{\mathcal{H}}_z \quad (7)$$

where $\hat{\mathcal{H}}_0$ is the zero field splitting, eq 2 $\hat{\mathcal{H}}_{ex}$ is the exchange interaction, eq 1 and

$$\hat{\mathcal{H}}_Z = \beta(\hat{S} \cdot \mathbf{g} + g'\hat{S}') \cdot \vec{B} \quad (8)$$

is the Zeeman interaction. The radical is supposed to have spin-only paramagnetism, $g' \simeq 2$, while the ferryl iron has a $\mathbf{g}$ tensor that can be related to the zero field splitting (Oosterhuis & Lang, 1973). For axial symmetry we have, in second-order perturbation

$$g_\parallel = 2 - 4(D/\zeta)^2 \qquad g_\perp = 2 + 4D/\zeta + 8(D/\zeta)^2 \quad (9)$$

where $\zeta \approx 400$ cm^{-1} is the one-electron spin-orbit coupling

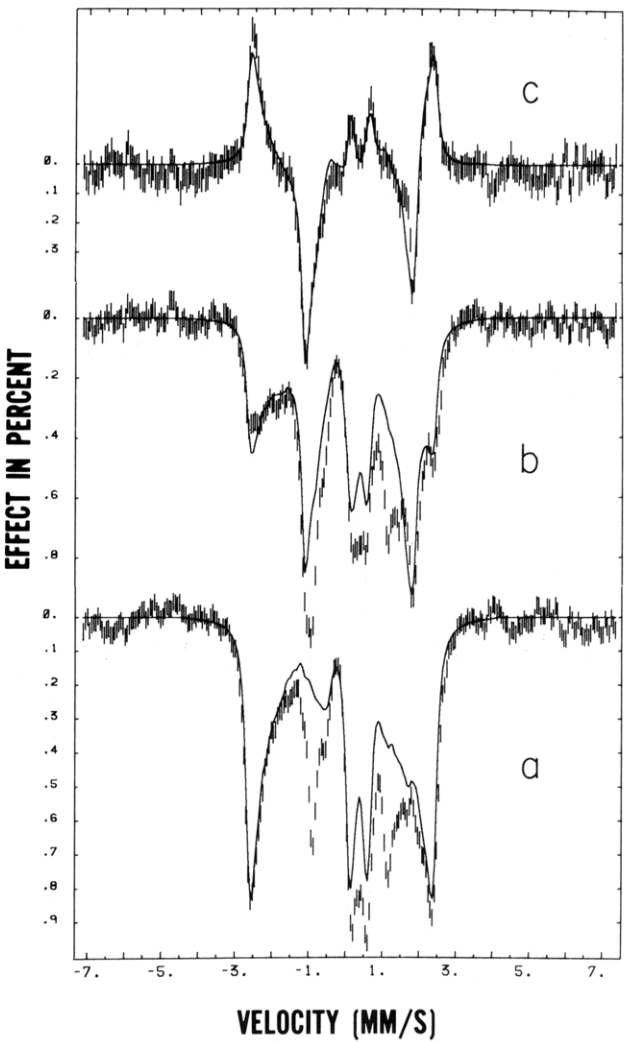

FIGURE 7: Mössbauer spectra of chloroperoxidase compound I. The spectra were taken at 4.2 K in an applied field of 34 mT (a) parallel and (b) perpendicular to the direction of the beam of gamma rays. In both traces the spectral contribution of the native enzyme has been subtracted. Trace c is the difference spectrum, (c) = (b) − (a). The solid line represents the simulation discussed in the text.

[4] The area near $v = 0.3$ mm/s may represent a heme decay product. If the remaining two lines form a doublet, the quadrupole splitting $\Delta E_Q \sim 2.2$ mm/s and the isomer shift $\delta_{Fe} \sim 0.1$ mm/s are outside the range observed for ferryl porphyrins (1.03 mm/s $\leq \Delta E_Q \leq$ 1.61 mm/s, 0.03 mm/s $\leq \delta_{Fe} \leq$ 0.11 mm/s, 0.03 mm/s $\leq \delta_{Fe} \leq$ 0.11 mm/s) or for O_2 adducts (2.11 mm/s $\leq \Delta E_Q \leq$ 2.31 mm/s 0.22 mm/s $\leq \delta_{Fe} \leq$ 0.27 mm/s) but close to the values reported for a dichlorocarbene complex of tetraphenylporphyrin, $\Delta E_Q = 2.28$ mm/s and $\delta_{Fe} = 0.10$ mm/s at 131 K (English et al., 1983).

[5] With the sign convention adopted here, $J < 0$ means ferromagnetic; $J > 0$, antiferromagnetic coupling.

Table I: Parameters of Chloroperoxidase Compound I and Related Systems Deduced from EPR and Mössbauer Data

	δ_{Fe} (mm/s)[d]	ΔE_Q (mm/s)[d]	$A_\perp/(g_n\beta_n)$ (T)[e]	D/k (K)	J	E/D
CPO I[a]	0.15	1.02	−20.2	52	$J = 1.02D$	0.035[f]
HRP I[b]	0.08	1.25	−19.3	37	$\|J\| \lesssim D/10$	~0
TMPIA[c]	0.06	1.62	−22.1	27	$-J > D$	0.067[g]

[a] Chloroperoxidase compound I (this work). [b] Horseradish Peroxidase compound I (Schulz et al., 1984). [c] Compound A of chloro-5,10,15,20-tetra(mesityl)porphinatoiron (Boso et al., 1983). [d] At 4.2 K, estimated uncertainty is ±0.01 mm/s. [e] Estimated uncertainty is ± 1 T. [f] Model-dependent, tentative values. [g] See footnote 8.

constant, and the symmetry axis is expected to be the heme normal. More general relations between D, E and $\mathbf{g}$ are obtained from exact numerical solutions.[6] Given a set of parameters, D, E, and $\mathbf{J}$, the calculation of the energy eigenvalues and the eigenfunctions of $\hat{\mathcal{H}}$ is straightforward. The $(2S + 1)(2S' + 1) = 6$ eigenfunctions form three Kramers doublets, which remain 2-fold degenerate in zero field. For axial symmetry and isotropic J, the eigenfunctions depend on the ratio J/D only, once the g values are specified. In general, the total spin of the system is not a good quantum number, but it is instructive to calculate the spin expectation values $\langle \mathbf{S} \rangle$ of the iron and $\langle \mathbf{S}' \rangle$ of the radical as a function of J/D.

As shown by EPR data, the lowest Kramers doublet is well separated in energy from the two higher ones and can thus be represented in terms of an effective spin $S^{eff} = {}^1/_2$ with eigenfunctions $|1/2, \pm 1/2)$. If we label the S^{eff} eigenfunctions of $\hat{\mathcal{H}}_0$ by $|i, \pm\rangle$ i = 0, 1, 2 and assume isotropic exchange, then we can define an effective $\mathbf{g}$ tensor, $\mathbf{g}^{eff}$, of the lowest Kramers doublet, $i = 0$, by

$$\langle 0, +|(\hat{S}\cdot\mathbf{g} + \hat{S}'g'\cdot\vec{B}|\ 0, \pm\rangle = \langle 1/2,\ 1/2|\hat{S}^{eff}\cdot\mathbf{g}^{eff}\cdot\vec{B}|1/2, \pm 1/2) \quad (10)$$

The Zeeman splitting in small field is then given by $\Delta E = \beta\{\sum(g_\nu^{eff}B_\nu)^2\}^{1/2}$, where the $(g_\nu^{eff})^2$ values are principal axes components of the tensor $(\mathbf{g}^{eff})^2$ and B_ν is the projection of $\vec{B}$ along the prinicpal axes ν. Figure 8 is a plot of the principal axes values $(g_x^{eff})^2 = (g_y^{eff})^2 = (g_\perp^{eff})^2$ and $(g_z^{eff})^2 = (g_\parallel^{eff})^2$ for isotropic J and $E = 0$ as a function of the parameter J/D, where the z axis is defined by the zero field splitting $\hat{\mathcal{H}}_0$, eq 2, and must represent the heme normal. The ferryl g values are taken to be $g_\perp = 2.28$ and $g_\parallel = 1.94$, which is appropriate for the case $D/k = 52$ K. Also shown are the spin expectation values $\langle S_\perp \rangle$, $\langle S_\parallel \rangle$ of the iron. Figure 8 succinctly summarizes the basic features of the spin-coupling model. The effective g value along the heme normal is essentially constant for all values of J/D, $g_\parallel^{eff} \approx 2$, while $g_\perp^{eff}$, which characterizes the magnetic moment in the heme plane, varies substantially with J/D. For antiferromagnetic coupling, $J > 0$, $g_\perp^{eff}$ passes through zero at $J/D \simeq 0.4$ (at $J/D = {}^4/_9$ for $g = g' = 2$), while it increases monotonically with J/D for ferromagnetic coupling, $J < 0$. The spin expectation values $\langle S_\perp \rangle$ and $\langle S_\parallel \rangle$ are zero for $J = 0$ and increase or decrease monotonically with J to reach saturation values ${}^2/_3$ for $J > 0$ and $\langle S_\perp \rangle = -{}^2/_3$, $\langle S_\parallel \rangle = {}^1/_3$ for $J < 0$ assuming $g = g' = 2$. We obtain an even greater variety of effective g values if we allow E to be finite and/or J to be anisotropic. In general, however, we expect E and the anisotropic terms of $\mathbf{J}$ to be small compared to D, $D/k \geq 30$ K (Osterhuis & Lang, 1973; Schulz et al., 1984); thus, Figure 8 should serve as a good first approximation. For the EPR data of chloroperoxidase compound I, $g_\parallel^{eff} = 2.0$ and $g_\perp^{eff} \approx 1.73$, we find two solutions in Figure 8, one with $J/D = 1.02$,[7] another one with $J/D = 0.057$. We can rule out the second one on the basis of the Mössbauer results. In the effective spin representation ($S^{eff} = {}^1/_2$) we found $A_\perp^{eff}/(\beta_N g_N) = -30$ T and $A_\parallel^{eff}/(\beta_N g_N) = -6$ T. The parameters of other ferryl compounds referred to the intrinsic iron spin ($S = 1$), however, are found to be $A_\perp/(\beta_N g_N) \sim -20$ T and $A_\parallel/(g_N\beta_N) \sim -6$T (Boso et al., 1983). To make the more accurately known $A_\perp$ compatible with $A_\perp^{eff}$ of chloroperoxidase compound I, we have to set $\langle S_\perp \rangle A_\perp \approx \langle S_\perp^{eff} \rangle A_\perp^{eff} = A_\perp^{eff}/2$, which leads to $\langle S_\perp \rangle \simeq 0.75$ and thus favors the solution $J/D = 1.02$. To verify the consistency of the calculations, we have simulated the spectra of Figure 7 with the spin-coupled model of Schulz et al. (1979b) by using the intrinsic parameters listed in Table I. The resulting traces are indistinguishable from those in Figure 7.

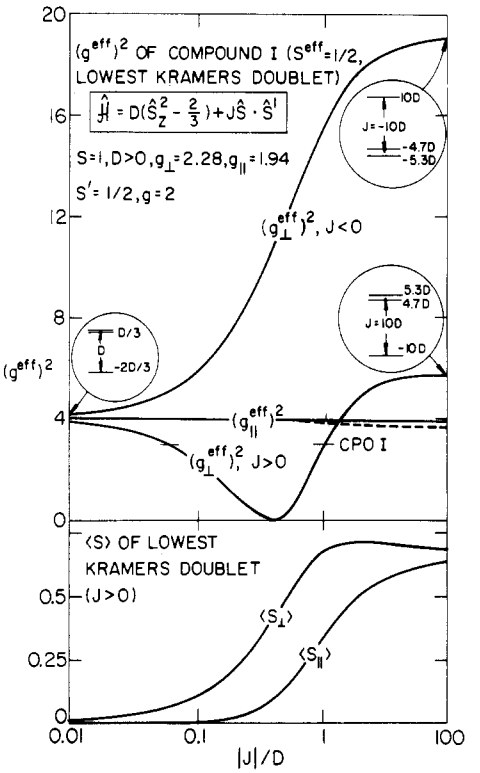

FIGURE 8: Spin-coupling model for primary compounds. The model assumes a positive axial zero field splitting D of the ferryl spin $S = 1$ and an isotropic exchange interaction between S and the porphyrin radical spin $S' = {}^1/_2$. The values adopted for the ferryl g tensor are those predicted for $D/k \approx 52$ K by the model of Oosterhuis & Lang (1973). The plot shows the squares of the effective g values, $(g_\perp^{eff})^2$ and $(g_\parallel^{eff})^2$, and the expectation values $\langle S_\perp \rangle$ and $\langle S_\parallel \rangle$ of the ferryl spin as a function of $|J|/D$ for the lowest Kramers doublet.

A more demanding test of the proper parametrization is the simulation of the EPR spectrum. Given $J/D = 1.02$ for chloroperoxidase compound I from the arguments of the last paragraph, we can calculate the energies of the excited

[6] In the simulation shown in Figure 5b, the values 2.28 ± 0.415 (E/D) were adopted for g_x and g_y as calculated from the model of Oosterhuis & Lang (1973) for $\Delta/\zeta = 3.4$, the ratio appropriate for chloroperoxidase compound I.

[7] This solution was suggested to us by Dr. B. Hoffman (private communication).

Kramers doublets to be E_1/D 1.56 and $E_2/D = 2.07$, as shown in the insert of Figure 6. If we identify the energy E_1 of the lower level with $k\Delta$,[2] $\Delta = 79.5$ K as found by fitting the spin relaxation data, we find $D/k = 52$ K, which is the largest value of any known ferryl state.

We searched for a best approximation of the spectrum in Figure 5 on the basis of the method used to model the compound I data of horseradish peroxidase (Schulz, 1979; Schulz et al., 1984). The model is specified by eq 7, and the assumption that the anisotropic effective line width, which is given as 17.5, 17.5, 5 mT in the caption of Figure 5, arises from a (Gaussian) distribution in one of the parameters. Considering the facts that the EPR difference spectrum in Figure 5 is not perfect and that it is impossible to determine the numerous parameters of eq 7 uniquely, we imposed a number of restrictions: We let the principal axes of all tensors coincide, calculated the ferryl **g** tensor as a function of D and E by using the approach of Oosterhuis & Lang (1973), and tried to model the line shape by distributing the (diagonal) exchange tensor **J** only. With these constraints, we found the best simulations to have small rhombicity, $E/D \simeq 0.035$, a small deviation of **J** from isotropy, $\mathbf{J}/k = 52, 52, 54$ K, and a small standard deviation, $\sigma(J)/k = 1.14$ K, of the Gaussian distribution. It should be pointed out that an intrinsic line width of 1 mT was assumed. The shape of the resulting simulation, Figure 5b, matches the data as well as we have reason to expect. While the parameter set is not unique, it is interesting to note that a comparable spread in J values was required to reproduce the compound I data of horseradish peroxidase.

In Table I we summarize the parameters of the green primary compounds analyzed so far. We include the results of Boso et al. (1983) on the green compound A of chloro-5,10,15,20-tetra(mesityl)porphinatoiron (TMP-A), which is an oxoferryl porphyrin cation radical complex like the primary compounds of chloroperoxidase and horseradish peroxidase but has, in contrast to the latter, an effective spin S^{eff} of $^3/_2$. TMP-A thus represents the first example of strong ferromagnetic coupling between the iron and the porphyrin radical ($J < 0$, $|J|/D \gg 1$ in Figure 8). In TMP-A the iron is presumably five-coordinated (Penner-Hahn et al., 1983) while it is six-coordinated in horse-radish peroxidase compound I. An axial histidine nitrogen and an ^{17}O ligand have been identified in horseradish peroxidase compound I by ENDOR (Roberts et al., 1981a,b). The axial iron ligands of chloroperoxidase compound I are presumed to be oxygen, as inferred from studies with $H_2{}^{18}O_2$ (Hager et al., 1972), and cysteinate, as suggested by EXAFS measurements on native chloroperoxidase (Cramer et al., 1978).

A comparison of the parameters listed in Table I with those of iron porphyrins in the compound II state (Schulz et al., 1984) confirms our basic model assumption that the intrinsic properties of the oxoferryl iron are independent of the presence or absence of exchange interaction. As predicted by the crystal field model of Oosterhuis & Lang (1973), the zero field splitting parameter D is large and positive and the deviations from axial symmetry are minor.[8] Computer simulations of the Mössbauer data are not sensitive to small rhombicities, and the assumption of axial symmetry leads to adequate solutions. They are compatible with the predictions of the crystal field model except for the quadrupole splittings, which are predicted to be $\Delta E_Q \sim 3$ mm/s while the observed values range from 1 to 1.6 mm/s. The crystal field model accounts for that part of the electric field gradient due to the t_{2g} valence electrons only and ignores the covalency contribution, which must be of comparable magnitude. Molecular orbital calculations predict quadrupole splitting closer to the empirical values (Loew & Herman, 1980).

The strength and sign of the exchange interaction apparently depends on structural details that must be further defined. A wide variety of magnetic phenomena can be expected on the basis of the spin-coupling model as illustrated in Figure 8. Horseradish peroxidase compound I with an EPR signal centered at $g = 2$ represents the weak coupling limit, $|J|/D < 0.1$, with small positive and negative J components, while the model complex, TMP-A, represents the strong coupling limit with g values near 2 and 4. Among the compounds I, chloroperoxidase is the first known case of intermediate coupling, $|J/D| \sim 1$, as deduced from the characteristic EPR and Mössbauer spectra. A reduction in J/D by a factor of 2.5, on the other hand, would lead to an EPR silent species ($g_\perp{}^{\text{eff}} \sim 0$) that could still show a magnetically split Mössbauer spectrum. It remains to be seen if the noted failure to observe an EPR signal in other primary compounds of peroxidase can be explained by this model.

[8] The **g** tensor of TMP-A implies $E/D = 0.067$ (B. Hoffman and J. T. Groves, private communication). Axially symmetric parameters are adequate to reproduce the Mössbauer spectra (Boso et al., 1983).

References

Ballou, D. P., & Palmer, G. A. (1974) *Anal. Chem. 46*, 1248–1253.

Boso, B., Lang, G., McMurray, T. J., & Groves, J. T (1983) *J. Chem. Phys. 79*, 1122–1126.

Champion, P. M., Münck, E., Debrunner, P. G., Hollenberg, P. F., & Hager, L. P. (1973) *Biochemistry 12*, 426–435.

Champion, P. M., Chiang, R., Münck, E., Debrunner, P. G., & Hager, L. P. (1975) *Biochemistry 14*, 4160.

Chance, B. (1950) *Biochem. J. 46*, 387–402.

Colvin, J. T., Rutter, R., Stapleton, H. J., & Hager, L. P. (1983) *Biophys. J. 41*, 105–108.

Cotton, M. L., Ragcheea, J. M. T., & Dunford, H. B. (1973) *Can. J. Biochem. 51*, 627–631.

Cramer, S. P., Dawson, J. H., Hager, L. P., & Hodgson, K. O. (1978) *J. Am. Chem. Soc. 100*, 7282–7290.

DiNello, R. K., & Dolphin, D. (1981) *J. Biol. Chem. 256*, 6903–6912.

Dolphin, D., Forman, A., Borg, D. C., Fajer, T., & Felton, R. H. (1971) *Proc. Natl. Acad. Sci. U.S.A. 68*, 614–618.

English, D. R., Hendrickson, D. N., & Suslick, K. S. (1983) *Inorg. Chem. 22*, 367–368.

Groves, J. T., Haushalter, R. C., Nakamura, M., Nemo, T. E., & Evans, B. J. (1981) *J. Am. Chem. Soc. 103*, 2884–2886.

Hager, L. P., Morris, D. R., Brown, F. S., & Eiberwein, H. (1966) *J. Biol. Chem. 241*, 1769–1777.

Hager, L. P., Doubek, D. L., Silverstein, R. M., Harges, J. H., & Martin, J. C. (1972) *J. Am. Chem. Soc. 94*, 4364.

Hoffman, B. M., Roberts, J. E., Brown, T. G., Kang, C. H., & Margoliash, E. (1979) *Proc. Natl. Acad. Sci. U.S.A. 76*, 6132–6136.

Hollenberg, P. F., & Hager, L. P. (1973) *J. Biol. Chem. 248*, 2630–2633.

Hollenberg, P. F., Hager, L. P., Blumberg, W. E., & Peisach, J. (1980) *J. Biol. Chem. 255*, 4801.

La Mar, G. N., & de Ropp, J. S. (1980) *J. Am. Chem. Soc. 102*, 395–397.

Lang, G., Spartalian, K., & Yonetani, T. (1976) *Biochim. Biophys. Acta 451*, 250–258.

Libby, R. P., Thomas, J. A., Kaiser, L. W., & Hager, L. P. (1982) *J. Biol. Chem. 257*, 5030–5037.

Loew, G. H., & Herman, Z. (1980) *J. Am. Chem. Soc. 102*, 6173-6174.
Morris, D. R., & Hager, L. P. (1966) *J. Biol. Chem. 248*, 7495-7498.
Oosterhuis, W. T., & Lang, G. (1973) *J. Chem. Phys. 58*, 4757-4765.
Palcic, M. M., Rutter, R., Araiso, T., Hager, L. P., & Dunford, H. B. (1980) *Biochem. Biophys. Res. Commun. 94*, 1123-1127.
Penner-Hahn, J. E., McMurry, T. J., Renner, M., Latos-Grazynsky, L., Smith-Eble, K., Davis, I. M., Balch, A. L., Groves, J. T., Dawson, J. H., & Hodgson, K. O. (1983) *J. Biol. Chem. 258*, 12761-12769.
Pichard, M. A. (1981) *Can. J. Microbiol. 27*, 1298-1305.
Roberts, J. E., Hoffman, B. M., Rutter, R., & Hager, L. P. (1981a) *J. Biol. Chem. 256*, 2118-2121.
Roberts, J. E., Hoffman, B. M., Rutter, R., & Hager, L. P. (1981b) *J. Am. Chem. Soc. 103*, 7654-7655.
Rutter, R., & Hager, L. P. (1982) *J. Biol. Chem. 257*, 7958-7961.
Schulz, C. E. (1979) Ph.D. Thesis, University of Illinois.
Schulz, C. E., & Debrunner, P. G. (1984) *Biophys. J. 45*, 2429.
Schulz, C. E., Chiang, R., & Debrunner, P. G. (1979a) *J. Phys., Colloq. (Orsay, Fr.) 40*, C2 534-536.
Schulz, C. E., Devaney, P. W., Winkler, H., Debrunner, P. G., Doan, N., Chiang, R., Rutter, R., & Hager, L. P. (1979b) *FEBS Lett. 103*, 102-105.
Schulz, C. E., Rutter, R., Sage, J. T., Debrunner, P. G., & Hager, L. P. (1984) *Biochemistry 23*, 4743-4754.
Shaw, P. D., & Hager, L. P. (1961) *J. Biol. Chem. 236*, 1626-1630.
Thomas, J. A., Morris, D. R., & Hager, L. P. (1970) *J. Biol. Chem. 245*, 3135-3142.
Wagner, G. C., & Gunsalus, I. C. (1981) in *The Biological Chemistry of Iron* (Dunford, D. B., Dolphin, D., Raymond, K., & Sieker, L., Eds.) Reidel, Boston.
Yim, M. B., Kuo, L. C., & Makinen, M. W. (1982) *J. Magn. Reson. 46*, 247-256.
Yonetani, T., Schleyer, H., & Ehrenberg, A. (1966) *J. Biol. Chem. 241*, 3240-3242.

Quasi-Elastic Light-Scattering Studies of Conformational States of the H,K-ATPase. Intervesicular Aggregation of Gastric Vesicles by Disulfide Cross-Linking†

M. Morii, N. Ishimura, and N. Takeguchi*

ABSTRACT: The particle size of hog gastric vesicles which contain H,K-ATPase was measured by using the method of quasi-elastic light scattering. The size of control vesicles is homogeneous as judged from its low polydispersity index. When the vesicles were treated with copper(II) *o*-phenanthroline (CuP), intervesicular S–S cross-linking occurred as determined by the aggregated vesicle size. The aggregation to divesicle size occurred very quickly, within 30 s, and the extent of aggregation did not depend on the extent of inactivation if the inactivation was not more than about 30%. Blocking of SH groups by 5,5′-dithiobis(2-nitrobenzoic acid) in the presence of Mg^{2+} prevented CuP-induced vesicular aggregation but not inactivation, indicating that S–S cross-linking rather than enzyme inactivation is the primary cause of vesicular aggregation. The presence of Mg^{2+} was required for the occurrence of aggregation. Nucleotides such as ADP ($K_{0.5}$ = 5 μM) and 5′-adenylyl imidodiphosphate ($K_{0.5}$ = 50 μM) inhibited the aggregation induced by 50 μM CuP plus 2 mM Mg^{2+} in a dose-dependent manner. Furthermore, K^+ antagonized the effects of nucleotides. The extent of aggregation increased as the pH decreased in the pH range 6.1–7.4. Virtually no cross-linking occurred at alkaline pH (e.g., pH 8–9). These data show that vesicular aggregation can be assumed to reflect the conformational state of the responsible SH group in the native enzyme.

Gastric H,K-ATPase is involved in gastric acid secretion, and the presence of the enzyme is specific to parietal cells (Ganser & Forte, 1973; Lee et al., 1974; Sachs et al., 1976). The enzyme is in gastric vesicles, and it has two different K^+ sites, an internal high-affinity site and an external low-affinity site: the external low-affinity K^+ site is competitive with ATP (Wallmark & Mardh, 1979; Wallmark et al., 1980). It has been proposed that the ATPase assumes different conformational states depending on the presence of different ligands, e.g., K^+, nucleotides, and Mg^{2+} (Schrijen et al., 1980, 1981; Van de Ven et al., 1981; Jackson et al., 1983). These pieces of information were obtained by measuring changes in inactivation by chemical modification, nucleotide binding, and fluorescence probe studies. Although conformational changes have been proposed, they have not been unequivocally established. Therefore, it is worth further study by using different, especially new methods.

In this paper, we introduce a new method to obtain information about conformational states of membrane-bound enzymes. Using copper(II) *o*-phenanthroline (CuP),[1] which

† From the Faculty of Pharmaceutical Sciences, Toyama Medical and Pharmaceutical University, Toyama 930-01, Japan. *Received July 13, 1984.* This work was supported by grants from the Ministry of Education, Science and Culture, Japan and Takeda Science Foundation, Osaka.

[1] Abbreviations: CuP, copper(II) *o*-phenanthroline; AMPPNP, 5′-adenylyl imidodiphosphate; QELS, quasi-elastic light scattering; Nbs_2, 5,5′-dithiobis(2-nitrobenzoic acid); Pipes, piperazine-*N*,*N*′-bis(2-ethanesulfonic acid); $NaDodSO_4$, sodium dodecyl sulfate; kDa, kilodalton(s); Tris-HCl, tris(hydroxymethyl)aminomethane hydrochloride; EDTA, ethylenediaminetetraacetic acid.

0006-2960/84/0423-6816$01.50/0